

Quantum state tomography of a single electron spin in diamond with Wigner reconstruction

Bing Chen,^{1,2} Jianpei Geng,¹ Feifei Zhou,¹ Lingling Song,¹ Heng Shen,^{3,*} and Nanyang Xu^{1,†}

¹*School of Electronic Science and Applied Physics,
Hefei University of Technology, Hefei, Anhui 230009, China*

²*State Key Laboratory of Quantum Optics and Quantum Optics Devices,
Shanxi University, Taiyuan, 030006, China*

³*Clarendon Laboratory, University of Oxford, Parks Road, Oxford, OX1 3PU, UK*

(Dated: July 17, 2018)

We present the experimental reconstruction of the Wigner function of an individual electronic spin qubit associated with a nitrogen-vacancy (NV) center in diamond at room temperature. This spherical Wigner function contains the same information as the density matrix for arbitrary spin systems. As an example, we exactly characterize the quantum state of a single qubit undergoing a nearly pure dephasing process by Wigner function. The fidelities and purities during this process are extracted from the experimental reconstructed Wigner functions, whose dynamics agree with the theoretical prediction. Our method can be applied to multi-qubit systems for measuring the Wigner function of their collective spin state.

Quantum state tomography of a system from measurements is an important topic in the emerging field of quantum technology. Through full state reconstruction, one can estimate the properties of quantum systems such as entanglement and purity, and furthermore determine their potential application in fields of quantum metrology[1–6], quantum simulation[7–9] and quantum computation[10–16]. The most common method for full characterization of any quantum state is the density matrix reconstruction. However, as the number of qubits increases, the density matrix reconstruction with maximum likelihood estimation[17] in practice becomes problematic.

As a counterpart of density matrix reconstruction, the Wigner function was originally proposed for describing quantum systems with continuous degrees of freedom, for instance the harmonic-oscillator phase-space description of electromagnetic fields[18]. Many efforts have been made to generalize the method of the Wigner function to quantum systems with a finite-dimensional Hilbert space[19–29], such as systems of arbitrary angular momentum in spherical phase space. However, a complete reconstruction of the Wigner function in solid-state spin systems has not been experimentally realized.

Generally, as for spin system consisting of N atoms, with each atom representing a pseudo-spin-1/2 subsystem, the corresponding Wigner function is given as[19–21]

$$W(\theta, \phi) = \sqrt{\frac{2}{\pi}} \sum_{k=0}^{2j} \sum_{q=-k}^k Y_{kq}(\theta, \phi) \rho_{kq}, \quad (1)$$

where $j = N/2$ is the total spin length, and Y_{kq} are the usual spherical harmonics. θ is the polar angle measured from the +z-axis, and ϕ is the azimuthal angle around the z-axis. Here, the density matrix ρ is transformed from j-space (the Dicke representation $\rho_{mm'} = \langle m | \rho | m' \rangle$

of the density matrix) to k-space (the spherical harmonic decomposition ρ_{kq} by $\rho_{kq} = \sum_{m=-j}^j \sum_{m'=-j}^j \rho_{mm'} t_{kq}^{jmm'}$ with multipole operator-related coefficient $t_{kq}^{jmm'} = (-1)^{j-m-q} \langle j, m; j, -m' | k, q \rangle$, where $\langle j, m; j, -m' | k, q \rangle$ is Clebsch Gordan coefficient. This Wigner function contains the same information as the density matrix for any spin- j system, further, the expectation value of the angular momentum vector is proportional to the center of mass of the Wigner function, $\langle J_i \rangle = \sqrt{\frac{j(j+1)(2j+1)}{4\pi}} \int_0^\pi \sin(\theta) d\theta \int_0^{2\pi} d\phi f_i(\theta, \phi) W(\theta, \phi)$, where $i = (x, y, z)$ while $f_i(\theta, \phi) = \{\sin \theta \cos \phi, \sin \theta \sin \phi, \cos \theta\}$.

In this letter, we experimentally reconstruct the complete and continuous Wigner functions for the states of the electron spin of an NV center in diamond. Experiencing a nearly pure dephasing process, it is demonstrated that the decay of the fidelities and purities extracted from the reconstructed Wigner functions is in accordance with the dephasing time measured by a Ramsey sequence[30, 31]. Additionally, the minimum value of the Wigner function (W_{min}) is presented, which increases from negativity to positivity with the electron spin dephasing into a more and more mixed state. The negativity completely vanishes when the purity of the spin state extracted from the Wigner function is less than 2/3 which is the main conclusion of Ref[29]. However, due to the limited slices of Wigner function, the authors obtained the purity from typical density matrix reconstruction in that work.

The quantum-mechanical state of any two-level system can be expressed as a 2×2 density matrix $\rho = \frac{1}{2}(\mathbb{I} + \mathbf{r} \cdot \hat{\sigma})$ with the vectors $\mathbf{r} = (x, y, z) \in \mathbb{R}^3$ ($\|\mathbf{r}\| = \sqrt{x^2 + y^2 + z^2} \leq 1$) and Pauli operators $\hat{\sigma} = (\hat{\sigma}_x, \hat{\sigma}_y, \hat{\sigma}_z)$. To visualize the spin state pointing on the surface of Bloch Sphere, \mathbf{r} is typically represented as $\mathbf{r} = r \cdot (\sin \epsilon \cos \eta, \sin \epsilon \sin \eta, \cos \eta)$ where ϵ and η are the polar and azimuthal angle, respectively. Inserting this density

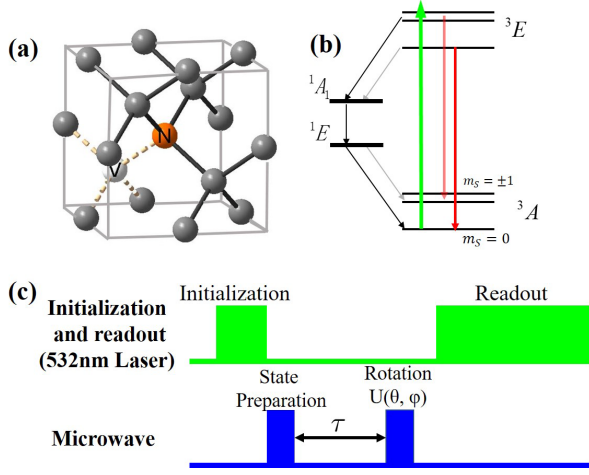


FIG. 1. (color online). (a) Atomic structure of NV center in diamond. The NV center in diamond which consists of a substitutional nitrogen atom (N) associated with a vacancy (V) in an adjacent lattice site of the diamond matrix[32], has C_{3v} symmetry. (b) Scheme of energy levels of the NV center electron spin. Its ground state (3A_2) and excited state (3E) are both spin triplet, and the transition between the two states is corresponding to the zero-phonon line(ZPL) at 637nm (1.945eV). The ground state (3A_2) is a spin triplet with zero-field splitting of 2.87GHz between $m_s = 0$ and $m_s = \pm 1$ states. The excited states(3E) is governed by spin-orbit and spin-spin interactions, split by 1.43GHz between $m_s = 0$ and $m_s = \pm 1$ states, all excited states spin levels (spin quantum number $m_s = 0, \pm 1$) exhibit spontaneous decay by photon emission. (c) The laser and microwave pulse sequence for the measurement of the Wigner function. The second microwave pulse corresponds to the unitary operation $U(\theta, \phi) = e^{-i\theta/2(\cos\phi\sigma_x + \sin\phi\sigma_y)}$. τ is the dephasing time.

matrix of single qubit to Eq.1, one can achieve the theoretical Wigner function for single qubit as follows,

$$W(\theta, \phi) = \frac{1 - \sqrt{3}r[\sin\epsilon \sin\theta \sin(\eta - \phi) + \cos\epsilon \cos\theta]}{2\pi^2}. \quad (2)$$

In general, due to connecting to the environment bath spin states experience a complicated decoherence process that contains both dissipative and dephasing dynamics. To clarify the dynamics of Wigner function of the single qubit, we experimentally prepare the spin state along y -axis as $|y\rangle = \frac{|0\rangle + i|1\rangle}{\sqrt{2}}$, i.e. $\epsilon = \pi/2, \eta = \pi/2$, which mainly suffers from the dephasing dynamics.

In the experiment, we use a purpose-built confocal microscopy to address and detect single nitrogen-vacancy centers in a type-IIa, single-crystal synthetic diamond sample (Element Six)[32]. The atomic structure and energy levels of the NV center in diamond are schematically shown in Fig.1a and Fig.1b, respectively. By applying a laser pulse of 532 nm wavelength with the assistance of intersystem crossing (ISC) transitions, the spin state can be polarized into $m_s = 0$ in the ground state(3A_2).

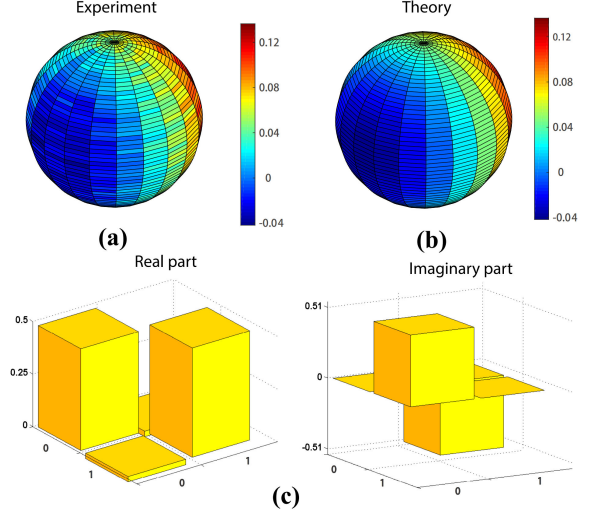


FIG. 2. (color online). Experimental (a) and theoretical (b) spherical Wigner function $W(\theta, \phi)$ of a qubit in state of $|y\rangle = (|0\rangle + i|1\rangle)/\sqrt{2}$ reconstructed on the curved Bloch sphere. θ is the polar angle measured from the $+z$ -axis, and ϕ is the azimuthal angle around the z -axis. (c) Real and imaginary parts, respectively, of the reconstructed density matrix elements of the qubit state. Each data point has been averaged 10^6 repetitions. The error bars account for the statistical error associated with the photon counting.

This process can be utilized to initialize and read out the spin state of the NV center. The fluorescence photons are detected by using the single photon counting module (SPCM). Additionally, a small permanent magnet in the vicinity of the diamond (magnetic field $B \approx 520G$) that is aligned parallel to the symmetry axis of the nitrogen vacancy center splits the $m_s = \pm 1$ spin levels. With this magnetic field, the ${}^{14}N$ nuclear spin of the NV center can be also polarized with the laser pulse[33]. It is observed in the optically detected magnetic resonance (ODMR) spectra that the nuclear spin polarization is higher than 98%. We encode $m_s = -1$ and $m_s = 0$ in 3A_2 as $|0\rangle$ and $|1\rangle$ of the electron spin qubit. The state of the qubit can be manipulated with microwave pulses(1404.3MHz), while the spin level $m_s = 1$ remains idle due to large detuning.

To make the Wigner function Eq. 2 more closely linked to the experimental implementation, we rewrite it as

$$\begin{aligned} W(\theta, \phi) &= \sqrt{\frac{2}{\pi}} \sum_{m=-j}^j p_m(\theta, \phi) R_{mj}, \\ R_{mj} &= \sum_{k=0}^{2j} \sqrt{\frac{2k+1}{4\pi}} t_{k0}^{jmm} \\ &= \frac{(-1)^{j-m}}{\sqrt{4\pi}} \sum_{k=0}^{2j} (2k+1) \binom{j}{m} \binom{j}{-m} \binom{k}{0}, \end{aligned} \quad (3)$$

where $p_m(\theta, \phi)$ is the spin projection probabilities pro-

jected along a specific quantization axis (θ, ϕ) with $\sum_{m=-j}^j p_m = 1$. And the coefficient R_{mj} is written in terms of a Wigner 3j-symbol. Based on the experimental equation, we can reconstruct the Wigner function of the spin state from experimental result.

For each experimental cycle of Wigner function reconstruction as shown in Fig.1c, we start the sequence with $1\mu\text{s}$ of laser illumination to polarize the nitrogen-vacancy electron spin and nearby nuclear spins into state $|1\rangle$. Then the qubit is prepared into state $(|0\rangle + i|1\rangle)/\sqrt{2}$ by a $\pi/2$ microwave pulse. An idle time of τ is followed, during which the qubit dephases into a mixed state. For the measurement of the Wigner function of the state, we apply a second microwave pulse with phase ϕ , Rabi frequency Ω_W , and duration θ/Ω_W . The second microwave pulse thus corresponds to the unitary operation $e^{-i\theta/2(\cos\phi\sigma_x + \sin\phi\sigma_y)}$. After the microwave pulse, another $1\mu\text{s}$ laser pulse is applied and fluorescence emission is detected by the single photon counting module and be normalized into the population of state $|1\rangle$ and $|0\rangle$. We can obtain the expectation of $p_m(\theta, \phi)$ and reconstruct exactly the experimental Wigner function basing on Eq.3. To reconstruct the Wigner function, we vary θ from 0 to π with a step of $\pi/60$ and ϕ from 0 to 2π with a step of $\pi/10$. The variation of θ and ϕ is realized by varying the duration and phase of the microwave pulse, which is generated from an IQ-modulation system where we use an arbitrary waveform generator (Tektronix AWG510) to synthesize different frequencies and phases. The generated microwave pulse is passed through a switch, amplified by a power amplifier, and delivered by an impedance-matched coplanar waveguide (CPW) before being applied on the qubit.

Fig.2a presents the spherical Wigner function for the state $\rho_0 = |y\rangle\langle y|$ experimentally prepared at the initial time. The color on the Bloch sphere indicates the value of $W(\theta, \phi)$. As comparison, Fig.2b shows the theoretical Wigner function based on Eq.2 which agrees with the experimental Wigner function in Fig.2a. The density matrix of the spin state via standard quantum state tomography is shown in Fig.2c, with $\rho_{0,\text{exp}} = \begin{pmatrix} 0.482 \pm 0.014 & -0.026 \pm 0.018 - i(0.518 \pm 0.013) \\ -0.026 \pm 0.018 + i(0.516 \pm 0.013) & 0.518 \pm 0.014 \end{pmatrix}$.

As the state evolves in the dephasing process, the state becomes more and more mixed. Starting from the ideal initial state ρ_0 , the state should evolve as $\rho(\tau) = \frac{1}{2} \begin{pmatrix} 1 & -i\exp[-(\tau/T_2^*)^2] \\ i\exp[-(\tau/T_2^*)^2] & 1 \end{pmatrix}$ [34], where T_2^* is the dephasing time. We apply Ramsey sequence on the electron spin to measure T_2^* . The Ramsey sequence is $\pi/2 - \tau - \pi/2$ which is shown in the inset of Fig.3b). The dephasing time $T_2^* = 2.64 \pm 0.06\mu\text{s}$ can be obtained by fitting of the experimental Ramsey signal shown as the red circles in Fig.3b. We use fidelity and purity of the state to evaluate this dephasing dynamics. The fidelity and purity of the state $\rho(\tau)$ are defined as $F = (\text{Tr}(\sqrt{\sqrt{\rho_0}\rho(\tau)\sqrt{\rho_0}}))^2$ and $P = \text{Tr}(\rho(\tau)^2)$, which gives $F = 0.5 + 0.5\exp[-(\tau/T_2^*)^2]$

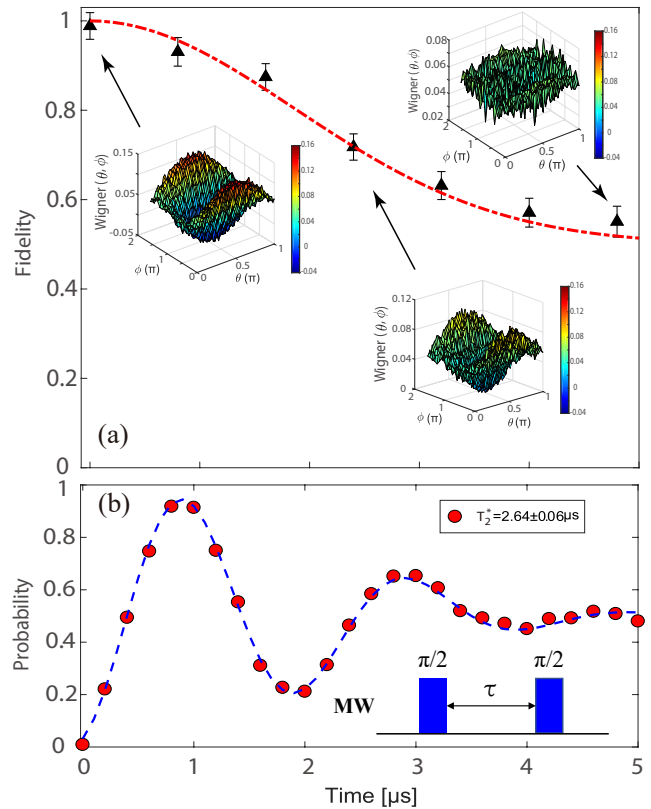


FIG. 3. (color online). (a) Dynamics of the Wigner function-extracted fidelity in a nearly pure dephasing process. The black triangle represents the fidelity extracted from experimental Wigner function. The dashed line is the theoretical prediction. The three insets are the surface-plotted Wigner function (W_τ) at time $\tau = 0\mu\text{s}$, $2.4\mu\text{s}$ and $4.8\mu\text{s}$. (b) The Ramsey oscillation of the electron spin coherence. The data were taken with the microwave detuning of 0.5 MHz by varying the temporal separation between the two microwave $\pi/2$ pulses. The Ramsey signal (red circle) was fitted to $\exp[-(\tau/T_2^*)^2] \cos(2\pi ft)$ (blue line) [30, 31] where f values correspond to the microwave detuning, obtained $T_2^* = 2.64 \pm 0.06\mu\text{s}$. The inset is the experimental microwave pulse sequence of the electron-spin free precession. Each data point has been averaged 10^6 repetitions. The error bars account for the statistical error associated with the photon counting.

and $P = 0.5 + 0.5\exp[-2(\tau/T_2^*)^2]$ as theoretical prediction. In the language of Wigner functions, they can be expressed as $F = 2\pi \int_0^\pi \sin(\theta) d\theta \int_0^{2\pi} d\phi W_\tau(\theta, \phi) W_0(\theta, \phi)$ and $P = 4\pi \int_0^\pi \sin(\theta) d\theta \int_0^{2\pi} d\phi W_\tau^2(\theta, \phi)$, where W_τ and W_0 are the Wigner functions corresponding to $\rho(\tau)$ and ρ_0 , respectively. Fig.3a and Fig.4a show the fidelity and purity extracted from the experimental Wigner function W_τ which are in good agreement with the theoretical predictions.

Further, we find that the Wigner function of the prepared initial state has negative region and W_{\min} in-

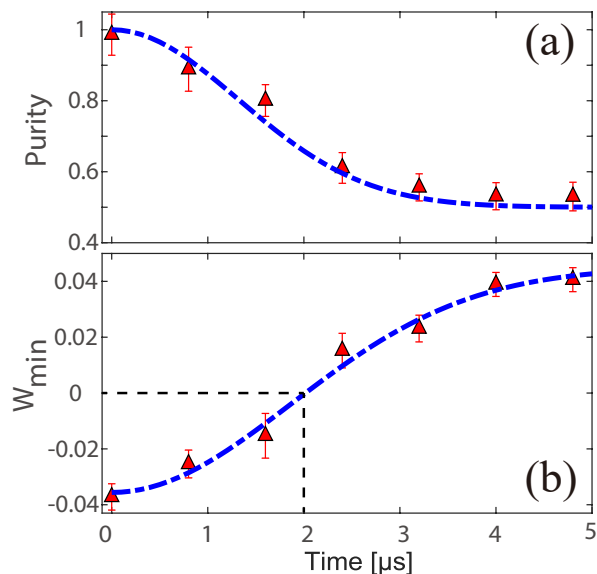


FIG. 4. (color online). (a) Dynamics of the Wigner function-extracted purity in a nearly pure dephasing process. The red triangle is the extracted purity, and the blue dashed line is theoretical prediction. (b) Measured W_{min} in a nearly pure dephasing process. The red triangle is the experimental data, and the blue dashed line represents a theoretical curve $\frac{1-\sqrt{3} \exp[-2(\tau/T_2^*)^2]}{2\pi^2}$ derived from Eq.2. Each data point has been averaged 10^6 repetitions. The error bars account for the statistical error associated with the photon counting.

creases gradually. As expected as the simulation (Eq.2) (Fig.4b), the negativity of the Wigner function completely vanishes around $2.0\mu s$ when the purity of the spin state extracted from the Wigner function is less than $2/3$, in agreement with the main observation in Ref[29].

In conclusion, we report the experimental reconstruction of the spherical Wigner function of a single qubit state for an NV center in a bulk diamond. In a nearly pure dephasing process, Wigner functions at different time are measured to extract the dynamical information of the spin states. We present the dynamics of the Wigner function-extracted fidelity and purity whose behavior agrees with the theoretical prediction. Our method can be applied to multi-spin systems for quantum state tomography instead of density matrix reconstruction, which is problematic in large spin systems.

The authors are grateful to Jie Li and Yanqiang Guo for fruitful discussions. The authors acknowledge financial support by the National Natural Science Foundation of China (grant No. 11604069, 61376128), by the National Key R&D Program of China(Grants No. 2018YFA0306600), the Anhui Natural Science Foundation (grant No. 1708085QA09), the Program of State Key Laboratory of Quantum Optics and Quantum Optics Devices(No.KF201802) and the Fundamental Research Funds for the Central Universities. H. Shen acknowledges

the financial support from the Royal Society Newton International Fellowship (NF170876) of UK.

* heng.shen@physics.ox.ac.uk

† nyxu@hfut.edu.cn

- [1] C. L. Degen, F. Reinhard, and P. Cappellaro, *Rev. Mod. Phys.* 89, 035002 (2017).
- [2] S. Zaiser, T. Rendler, I. Jakobi, T. Wolf, S.-Y. Lee, S. Wagner, V. Bergholm, T. Schulte-Herbruggen, P. Neumann, and J. Wrachtrup, *Nature communications* 7, 12279 (2016).
- [3] T. Unden, P. Balasubramanian, D. Louzon, Y. Vinkler, M. Plenio, M. Markham, D. Twitchen, A. Stacey, I. Lovchinsky, A. Sushkov, M. Lukin, A. Retzker, B. Naydenov, L. McGuinness, and F. Jelezko, *Phys. Rev. Lett.* 116, 230502 (2016)
- [4] J. Appel, P. J. Windpassinger, D. Oblak, U. B. Hoff, N. Kjergaard and E. S. Polzik, *Proc. Natl Acad. Sci. USA* 106 10960 (2010).
- [5] M. H. Schleier-Smith, I. D. Leroux and V. Vuletić, *Phys. Rev. Lett.* 104 073604 (2010).
- [6] C. Gross, T. Zibold, E. Nicklas, Estève J and M. K. Oberthaler, *Nature (London)* 464,1165 (2010).
- [7] A. Friedenauer, H. Schmitz, J. T. Glueckert, D. Porras and T. Schaetz, *Nat. Phys.* 4 757(2008).
- [8] K. Kim, M.-S. Chang, S. Korenblit, R. Islam, E. E. Edwards, J. K. Freericks, G.-D. Lin, L.-M. Duan and C. Monroe, *Nature (London)* 465, 590 (2010).
- [9] B. P. Lanyon, C. Maier, M. Holzäpfel, T. Baumgratz, C. Hempel, P. Jurcevic, I. Dhand, A. S. Buyskikh, A. J. Daley, M. Cramer, M. B. Plenio, R. Blatt and C. F. Roos, *Nat. Phys.* 13, 1158 (2017).
- [10] P. Neumann, N. Mizuochi, F. Rempp, P. Hemmer, H. Watanabe, S. Yamasaki, V. Jacques, T. Gaebel, F. Jelezko, and J. Wrachtrup, *Science* 320, 1326 (2008).
- [11] T. H. Taminiau, J. Cramer, T. van der Sar, V. V. Dobrovitski, and R. Hanson, *Nature nanotechnology* 9, 171 (2014).
- [12] T. Taminiau, J. Wagenaar, T. Van der Sar, F. Jelezko, V. V. Dobrovitski, and R. Hanson, *Phys. Rev. Lett.* 109, 137602 (2012).
- [13] F. Kong, C. Ju, Y. Liu, C. Lei, M. Wang, X. Kong, P. Wang, P. Huang, Z. Li, F. Shi, L. Jiang, and J. Du, *Phys. Rev. Lett.* 117, 060503 (2016).
- [14] K. Xu, T. Xie, Z. Li, X. Xu, M. Wang, X. Ye, F. Kong, J. Geng, C. Duan, F. Shi, and J. Du, *Phys. Rev. Lett.* 118, 130504 (2017).
- [15] D. Leibfried, E. Knill, S. Seidelin, J. Britton, R. B. Blakestad, J. Chiaverini, D. B. Hume, W. M. Itano, J. D. Jost, C. Langer, R. Ozeri, R. Reichle and D. J. Wineland, *Nature (London)* 438, 639 (2005).
- [16] J. Benhelm, G. Kirchmair, C. F. Roos and R. Blatt, *Nat. Phys.* 4 463 (2008).
- [17] M. Ježek, J. Fiurášek, and Z. Hradil, *Phys. Rev. A* 68, 012305 (2003).
- [18] A. I. Lvovsky and M. G. Raymer, *Rev. Mod. Phys.* 81, 229 (2009).
- [19] J. P. Dowling, G. S. Agarwal, and W. P. Schleich, *Phys. Rev. A*, 49, 4101 (1994).
- [20] R. Schmied and P. Treutlein, *New J. Phys.* 13, 065019

- (2011).
- [21] Robert McConnell, Hao Zhang, Jiazhong Hu, Senka Ćuk and Vladan Vuletić, *Nature*, 519, 439 (2015).
- [22] W. K. Wootters, *Ann. Phys. (NY)* 176, 1 (1987).
- [23] U. Leonhardt, *Phys. Rev. Lett.* 74, 4101 (1995).
- [24] A. Vourdas, *Rep. Math. Phys.* 40, 367 (1997).
- [25] C. Miquel, J. P. Paz, and M. Saraceno, *Phys. Rev. A* 65, 062309 (2002).
- [26] M. F. Riedel, P. Böhi, Y. Li, T. W. Hänsch, A. Sinatra, and P. Treutlein, *Nature (London)* 464, 1170(2010).
- [27] T. Tilma, M. J. Everitt, J. H. Samson, W. J. Munro, and K. Nemoto, *Phys. Rev. Lett.* 117, 180401 (2016).
- [28] R. P. Rundle, P. W. Mills, T. Tilma, J. H. Samson, and M. J. Everitt, *Phys. Rev. A* 96, 022117 (2017).
- [29] Y. Tian, Z. Wang, P. Zhang, G. Li, Jie Li, and T. Zhang, *Phys. Rev. A* 97, 013840 (2018).
- [30] G. de Lange, Z. H. Wang, D. Rist, V. V. Dobrovitski, R. Hanson, *Science*, 330, 60-63 (2010).
- [31] L. Childress, M. V. Gurudev Dutt, J. M. Taylor, A. S. Zibrov, F. Jelezko, J. Wrachtrup, P. R. Hemmer, M. D. Lukin, *Science*, 314, 281-285 (2006).
- [32] M. W. Doherty, N B. Mansonb, P. Delaney, Fedor Jelezko, Jörg Wrachtrupe, L. C. L. Hollenberg, *Phys. Rep.*528, 1-45 (2013).
- [33] V. Jacques, P. Neumann, J. Beck, M. Markham, D. Twitchen, J. Meijer, F. Kaiser, G. Balasubramanian, F. Jelezko, and J. Wrachtrup, *Phys. Rev. Lett.* 102, 057403 (2009).
- [34] *Lecture Notes for Quantum Information*, John Preskill, California Institute of Technology (2015).